PAPER

Check for updates

Analysis of the effect of abiotic stressors on BVOC emissions from urban green infrastructure in northern Germany†

J. Feldner,[a] M. O. P. Ramacher, [ID] [a] M. Karl, [ID] *[a] M. Quante [ID] [a] and M. L. Luttkus[b]

Many plants are well known to emit biogenic volatile organic compounds (BVOCs). Under certain conditions BVOCs strongly enhance the photochemical formation of ozone (O_3) and impact the levels of atmospheric photo-oxidants. Urban environments under the influence of climate change may face an increasing risk of elevated ozone formation potentials, because abiotic stressors such as heat and drought can stimulate BVOC emissions. However, it is largely uncertain how a combination of heat episodes and reduced soil water potentials affects air quality in cities. The effect of abiotic stress on BVOC emissions and urban O_3 formation was assessed for the coastal metropolitan area of Hamburg in Germany during the vegetation period of 2018, characterized by remarkable drought and heat periods. BVOC emissions were modelled using the Model of Emissions of Gases and Aerosols from Nature (MEGAN) version 3 that accounts for several abiotic stresses. Isoprene is the single VOC with the highest share (~60%) in the BVOC emissions of the study area. Drought stress was identified as the most important abiotic stressor that modulates BVOC emissions in this area. Modelled biogenic emissions calculcated with MEGAN3 were included together with emissions of relevant anthropogenic sectors in simulations with the chemistry transport model EPISODE-CityChem to calculate ozone concentrations under a scenario of prolonged drought stress. As a major result we identified that isoprene concentrations in Hamburg were reduced by 65% (range 6% to 95%) under drought stress during the growing period compared to non-stress conditions. Reduction of isoprene concentrations due to drought stress spatially coincided with a reduction of ozone concentrations. To asses the importance of chemical reactions involved in the formation of ozone, concentrations of isoprene, methacryloyl peroxy nitrate (MPAN) and methacrolein (MACR) have been analysed. The drought stress effect on isoprene emissions led to reductions of MACR and MPAN by approximately 80% and 20%, respectively. Since a VOC limited regime is found presently for Hamburg, it is likely that further reductions in anthropogenic NO_x emissions and/or increased BVOC emissions driven by extended green infrastructure and long-term temperature increases may lead to an enhanced photochemical production of ozone in Hamburg in the future.

Environmental significance

All around the world cities are taking action to adapt to burdens in conjunction with climate change, often by strongly expanding the urban green infrastructure. Trees and other vegetation may also provide some disservices in polluted urban air through the emission of biogenic volatile organic compounds (BVOCs), mainly isoprene and terpenes. Our understanding of how increased heat and drought stress affects BVOC emissions and urban air quality is currently rather limited. We assess the impact of abiotic stressors on BVOC emissions and their contribution to ozone concentrations in a Northern Europe metropolis. Drought stress significantly reduced both emissions and concentrations of isoprene. An analysis of the chemical regime indicates that future increases of BVOC emissions driven by extended green infrastructure may lead to enhanced photochemical production of ozone.

[a]*Helmholtz Zentrum Hereon, Max-Planck-Str. 1, 21502 Geesthacht, Germany. E-mail: matthias.karl@hereon.de*

[b]*Leibniz Institute for Tropospheric Research e.V. (TROPOS), Permoserstr. 15, 04318 Leipzig, Germany*

1 Introduction

A notable impact of global climate change is the projected increase in frequency and intensity of extreme weather events for many regions in the world in the forthcoming decades.[1] Urban environments are already experiencing impacts of the climate crisis such as intense heat waves and prolonged

drought periods. As three quarters of the European population live in these endangered urban settings,[2] city governments have come up with climate change adaptation and mitigation strategies. Among other options, the potential of vegetation and particularly trees in forests and urban green infrastructure (UGI) to take up and store carbon dioxide (CO_2) is a well-known mitigation strategy.[3,4] Especially effective is the long-term removal of CO_2 *via* incorporation into plant structures and sequestration.[5] Besides mitigation, plants in urban areas are also used for climate adaption strategies. A positive effect of trees in the urban context is the reduction of the urban heat island effect, by lowering the ambient air temperature near the surface through shadowing effects and evapotranspiration.[6–8]

Nevertheless, besides positive effects in terms of climate change adaptation and mitigation for urban areas, the effect of trees and other vegetation on urban air quality is ambivalent.[9,10] Trees can directly remove air pollutants through different mechanisms, *e.g.* by deposition of air pollutants onto vegetation surfaces or green roadside barriers,[10] stomatal uptake,[11] or transfer to another medium, mainly soil or water.[12] Among the proposed UGI measures to improve urban air quality and to reduce urban GHG emissions are: establishing green corridors, roof greening, urban gardening, and the expansion of existing UGI, such as roadside trees, park areas and urban forests.[13,14] Air pollution abatement through vegetation is both an economic benefit and a strategy to reduce respiratory diseases.[10,15] Furthermore, park visitation has a positive impact on the cardiovascular system by lowering the systolic blood and pulse pressure[16] and especially during heat waves they can mitigate adverse heat related health effects *e.g.* exhaustion, concentration and sleep problems.[17] Therefore, urban green is considered a key provider for urban ecosystem services.

However, under certain circumstances, vegetation can lead to adverse impacts in urban areas. UGI can impair ventilation through reduced airflow which impacts pollutant transport and dispersion leading to aggregation and consequently higher concentrations.[18,19] Moreover, plants emit highly reactive biogenic volatile organic compounds (BVOCs) which influence the urban atmospheric composition and can enhance near-surface ozone (O_3) formation, as certain BVOCs are O_3 precursor substances.[10] Episodes with elevated ozone during summer are of specific interest since these are associated with exceedances of the World Health Organization (WHO) guideline concentration limits. In 2019, 29% of the EU-28 urban population has been exposed to O_3 levels above the maximum daily 8 hours mean (MDA8) EU target value of 120 μg m^{-3} and 97% above the WHO MDA8 guideline value of 100 μg m^{-3} [2]. Thus, especially with regard to near-surface O_3 concentrations in cities, vegetation can have positive and negative effects.

In general, BVOCs play an important role for atmosphere-biosphere interactions, directly influencing the oxidants and aerosols which are linked to air quality and climate.[20,21] BVOCs are emitted by both terrestrial and aquatic ecosystems that are involved in plant growth, reproduction, communication and defense.[22] Each plant species has their own blend of compounds, which can strongly vary between individuals and plant communities. On a global scale isoprene is by far the

BVOC with highest emissions[22,23] while for Germany monoterpenes are most frequently emitted.[21] Isoprene is produced as a by-product of photosynthesis and therefore only during daytime. Isoprene is not stored in plants. Besides BVOCs, anthropogenic volatile organic compounds (AVOCs) also influence air quality in urban areas. AVOCs originate for the most part from processes related to transport, production or combustion.[11] While the majority of global isoprene and monoterpene emissions are of biogenic origin, it should be noted that these compounds are also emitted by vehicles and other anthropogenic sources.[24–27] However, anthropogenic isoprene emissions are generally rather small compared to the biogenic emissions, even in urban areas.[28]

The amount of BVOCs emitted by different plant species is strongly influenced by abiotic stressors, such as droughts, heat waves, extreme cold, strong winds or elevated O_3 or CO_2 concentrations. While mild drought affects neither isoprene nor other BVOCs significantly, prolonged or heavy drought can rapidly decline these emissions due to declining photosynthetic activity.[28] An increase in temperature will enhance BVOC emissions for the most part. Thus, the emission of BVOCs is strongly connected to extreme events, which are projected to increase in frequency and severity due to climate change. Since abiotic stressors stimulate BVOC emissions, there is a risk of enhanced ozone formation in urban environments and their surrounding area during extreme (heat) events.

Currently it is highly uncertain whether the ozone uptake by trees outweighs their contribution to ozone production by BVOC emissions and how this relation will be affected in a future climate especially in urban areas.[10] Thus, it is necessary to identify and quantify impacts on O_3 levels in urban areas, which are related to vegetation in general, and particularly trees within the city and its surrounding.

Taking into account the positive and negative effects of vegetation on air quality, as well as their potential to act as integral part of climate change adaptation and mitigation strategies, green urban environments can be considered as "open-labs" to study the effects of climate change on BVOC emissions. Urban conditions such as the urban heat island (UHI) and air pollution are proxies for predicted future conditions, *e.g.* rising temperatures, CO_2 concentrations or prolonged drought periods.[11] But, measurement studies on BVOCs in urban areas in Central Europe are scarce.[29] However, there is rising evidence from regional[21,30–32] and urban-scale[32–37] air quality modeling studies, that BVOC emissions have the potential to contribute to urban O_3 formation by 14–60% under various climatic conditions.

Nevertheless, most of these studies do not account explicitly for urban-scale processes due to low grid resolutions or non-specific parametrizations of urban phenomena such as road traffic emissions, street canyons, and local point sources. Moreover, BVOC emission inventories in resolutions suitable for urban-scales incorporating urban green areas (parks, green belts, alley trees, *etc.*) are a rather new development, and necessary chemistry mechanisms to account for BVOC-O_3 interactions are not implemented in urban-scale chemistry transport models yet. To tackle the question of BVOC-O_3

© 2022 The Author(s). Published by the Royal Society of Chemistry

Environ. Sci.: Atmos., 2022, **2**, 1132–1151 | **1133**

interactions under prolonged drought and heat extreme conditions, which are projected to occur more frequently in the future, proper modeling capabilities are necessary.

Following, this study estimates the net impact of drought stress on isoprene and other BVOC emissions from vegetation in the urban area of Hamburg (DE) and its surroundings. For this purpose, we (1) modelled BVOC emissions under different stress scenarios with the MEGAN3 (Model of Emissions and Gases from Nature,[38,39]), which we (2) applied in the urban-scale Chemistry Transport Model EPISODE-CityChem.[40] Therefore, it was necessary to update the chemistry mechanism in EPISODE-CityChem for BVOC chemistry. The year 2018 was chosen for this study, because during this year strong drought and heat periods occurred in Europe,[41] and it is considered to be a representative year for near future scenarios. In response to the 2018 drought event, most ecologically and economically important tree species in temperate forests of Austria, Germany and Switzerland showed severe signs of drought stress.[42]

The area of Hamburg was chosen as an example for a city in northern Europe with predominant maritime influence, which in a changing climate is expected to face heat waves accompanied by droughts more frequently.[43] Furthermore, recent studies[44] revealed underestimations in O_3 formation in the urban area of Hamburg, which might indicate a lack in O_3 precursors possibly from BVOCs sources within the urban area and its surroundings. The vegetation cover in the region surrounding the city is dominated by non-irrigated arable land (see ESI S7, Fig. S7-2†). However, in the north-west pastures and in the south coniferous forests together with mixed forests dominate. Broad-leaved forests surround the city of Hamburg with highest abundance in the east. Within the city of Hamburg, numerous parks and green areas exist. Thus, implications of the BVOC-O_3 interaction by UGI or surrounding vegetation might support UGI air pollutant abatement and climate mitigation strategies in urban areas in similar environments. Furthermore, the results of this study could also be used for air quality improvement and climate mitigation strategies for urban areas in similar environments. The overall aim of this study is to assess the impact of drought stress on BVOC emissions in the Hamburg metropolitan region and to identify the resultant effect on ozone concentrations in the city of Hamburg.

In the following, we will briefly provide the theoretical description of BVOC emissions and chemistry necessary for an understanding of the BVOC-ozone interactions, before introducing the materials and methods of this study. This is followed by a presentation of results and their discussion.

2 Background theory

2.1 BVOC emission under no-stress conditions

BVOC emissions from vegetation occur either light- and temperature-dependent or only temperature-dependent. Light- and temperature-dependent emissions are linked to photosynthesis (synthesis emissions) while temperature-depended emissions occur for plants with storage capacity (pool emissions) throughout the day.[20] Next to isoprene, there are also light-depended monoterpene emissions but the majority of monoterpenes is emitted from storage pools inside plant properties as needles or leaves.[45] Sesquiterpenes and oxygenated BVOCs (OVOCs) are considered to be both light- and temperature-dependent.[23] There is a variety of parameters that influence BVOC emission response to environmental conditions. Some of these responses can be parameterized based on empirical constants, while others depend on plant as well as BVOC species-specific parameters (e.g., leaf area index, biomass density, standard emission potential). The main drivers are temperature, photosynthetic radiation and the seasonality. For pool emissions, the emission rate increases exponentially with temperature while for synthesis emission there is a threshold at around 314 K after which the emission declines.[46] This threshold may vary between tree and BVOC species and is additionally impacted by past environmental conditions.[20] Furthermore, the simulation of BVOC emission is highly sensitive to the underlying land use. In contrast to generalized land uses categories tree species-specific information will lead to more precise emission patterns[47] and in the case of Germany 50% lower BVOC (without OVOC) emissions.[21]

2.2 BVOC emission under stress conditions

Additionally, BVOC emissions are impacted by abiotic (heat, drought, ozone, nutrient availability, etc.) and biotic stressors (herbivores, pathogens) reducing certain BVOC emissions, while others increase and some of which are solely emitted during stress events.[12,20] For example, plant cell damage due to biotic stressors induces the emission of green leaf volatiles which are produced from fatty acids and comprises hexanal- and hexanol-derivatives.[20] When trees are exposed to sustaining drought conditions, the leaf temperature increases due to a decreasing transpiration rate. In chamber experiments, averaged leaf temperatures under drought conditions were reported to be 4 °C to 5 °C higher than the ambient temperature.[48] Due to a very quick fluctuation rate, leaf temperatures can occasionally exceed their ambient temperatures by even more than 10 °C for several seconds.[28] Drought conditions increase the diffusive resistance towards CO_2 entry into chloroplasts and thus down-regulate the photosynthesis rate.[49] Compounds with a high Henry's law constant (e.g., 7780 Pa m^3 mol^{-1} for isoprene or 13 600 Pa m^3 mol^{-1} for α-pinene) have a low dependence on stomatal conductance. Therefore, the increased partial pressure in case of stomatal closure compensates for the diffusion resistance. In contrast, compounds with a low Henry's law constant (e.g., 0.461 Pa m^3 mol^{-1} for methanol or 2.09 Pa m^3 mol^{-1} for linalool) partition more into the liquid phase in case of stomatal closure which leads to a long-term affection of emissions.[28]

Drought responses of BVOCs depend on the severity of drought stress, which can be defined by the degree of stomatal conductance. Here, a conductance level over 150 mmol H_2O m^{-2} s^{-1} is representing mild drought and a conductance level under 100 mmol H_2O m^{-2} s^{-1} is representing severe drought.[50] During drought conditions, the photosynthetic carbon input is blocked, but alternative carbon sources can compensate for

these reductions decoupling photosynthesis and isoprene production. The use of these alternative carbon sources stops once isoprene production and photosynthesis are re-coupled.[28] Furthermore, also the temperature dependence of isoprene is decoupled during and after severe drought stress.[51] Thus, mild drought may lead to slight increases in emissions, but severe drought leads to a decrease in emissions. Decreasing emissions can be ascribed to a general decrease in plant performance due to transpiration and net assimilation.[48]

2.3 BVOC impacts on air quality

Once emitted into the atmosphere BVOCs are quickly oxidized by ozone, hydroxyl (OH) and nitrate (NO_3) radicals while the reaction speed depends on the BVOC itself and the oxidizing partner. For a detailed description of BVOC chemistry we refer to Atkinson[52] and Atkinson & Arey.[53] In urban environments, concentrations of nitrogen oxides ($NO_x = NO + NO_2$) are high and here the photochemical ozone production is coupled to the NO_x cycle. The reaction of ozone with nitric oxide (NO) generates nitrogen dioxide (NO_2) and oxygen (O_2) and the subsequent photolysis of NO_2 regains NO and produces ground-state oxygen, which together with the O_2 regains the ozone. Between these reactions, a photostationary state is reached, which is disturbed in the presence of BVOC. The oxidation of BVOCs leads to the formation of organic peroxy radicals, which instead of ozone react with NO and produce NO_2. Furthermore, during the chemical degradation of BVOCs also the hydroperoxy (HO_2) radical is formed, which additionally converts NO to NO_2. Thus, the oxidation of BVOCs in high NO_x environments will increase ground-level ozone concentrations.

Another focus of this study are methacrolein (MACR) and peroxymethacryloyl nitrate (MPAN), which are both isoprene chemistry products. MACR is directly produced by the reaction of isoprene with ozone (IS-3 in ESITable S2-2,† which introduces the isoprene chemistry in EPISODE-CityChem). The oxidation by the OH radical (IS-1) and the NO_3 radical (IS-2) produces MACR after subsequent reaction with NO (IS-4, IS-11). The further oxidation of MACR by the OH radical (IS-6) and subsequent reaction with NO_2 (IS-21) will lead to MPAN formation. Therefore, MACR is linked to NO while MPAN is linked NO_2.

In addition, it should be stated, that the chemical degradation of BVOCs also leads to the formation of secondary organic aerosols (SOA), which is a component of fine particulate matter ($PM_{2.5}$)[54]. However, for Hamburg this is expected to play only a minor role.

For Germany, the main isoprene emitting tree species are oaks (*Quercus robur*, *Quercus rubra*, *Quercus petraea*) which is preferably oxidized by hydroxyl radicals and linked to ozone production.[21] Coniferous trees emit monoterpenes; the most common species are pine (*Pinus sylvestris*) and spruce (*Picea abies*). In addition, deciduous trees, mainly beech (*Fagus sylvatica*) show high monoterpene emission potentials. It is noteworthy, that the entire beech, most spruce and half of the pine monoterpene emissions are light depending. Monoterpenes are oxidized by ozone, OH and NO_3 radicals. Their impact on ozone is therefore ambivalent, but tree species with a high limonene

contribution are likely to facilitate ozone and SOA formation.[21] For Germany, the overall reduction of 50% in BVOC emissions lowers the average ozone concentration by 2.5% mainly due to reduced isoprene and limonene emissions and SOA by up to 60%.[21]

3 Materials, methods, developments

To identify the impact of different abiotic stressors, such as drought conditions, on urban-scale BVOC and O_3 concentrations, we applied an air quality modeling framework (Fig. 1).

The modeling framework applies the biogenic emissions inventory MEGAN3 to simulate biogenic emissions for different stress scenarios, which are transferred to the urban-scale Chemistry Transport Model Episode-CityChem.[40] Both models are driven by the same meteorological input of the COSMO-CLM v5.0.[55] In the following, the modeling setup will be briefly described and necessary developments to account for urban-scale BVOC representation in EPISODE-CityChem will be introduced.

3.1 Study area and study year

Hamburg is situated in the coastal Northern German lowland and thus controlled by a marine climate. In 2021 the average temperature of 9.8 °C was slightly above the national average of 9.3 °C in the most recent reference period (1991–2020).[43] Due to elevated greenhouse gas emissions in the past 100 years, the worldwide average air temperature has risen by approximately 0.7 °C,[56] in Hamburg it has risen by 1.7 °C since 1881.[43] Hamburg was also affected by the heat waves in 2018. Especially in the summer of 2018, the number of hot days (daily max. $T > 30$ °C) reached a record count of 16 days. There is no unique definition of a heat wave. For the Hamburg region the German weather service (DWD) reported a consecutive 14 days period in 2018 of extensively high temperatures with a mean daily maximum temperature 30.2 °C, which is labeled as heat wave.[57] Also for drought, there is no unique quantitative definition. Several institutions have developed certain drought indices. Here, the German drought monitor operated by Helmholtz Centre for Environmental Research[58] is consulted. It uses an operational modeling system that is based on a set of observational data. For July 2018, the soil moisture index for topsoil (uppermost 25 cm) was classified in the Hamburg area between severe drought and extreme drought. The entire monitored soil column (1.8 m) as was classified as moderate drought. The extremely hot and dry period lasted from April till October.[43] In terms of air quality, Hamburg frequently exceeds limit values of $PM_{2.5}$ and NO_2, especially at measurement stations near road traffic. Ozone concentrations in Hamburg reach only very rarely alarming levels.[59,60] During the study period, there was only one event (June 8 2–4 pm local time) where the threshold of 180 μg m^{-3} was exceeded. Almost 60% of Hamburg's area are used as traffic or settlement areas. In addition, there are several parks and green areas.[61] The total share of green urban areas (GUA) in Hamburg is 43.2%. Thereby, Hamburg stands alongside many European cities such as Amsterdam, Budapest, Helsinki, Lisbon
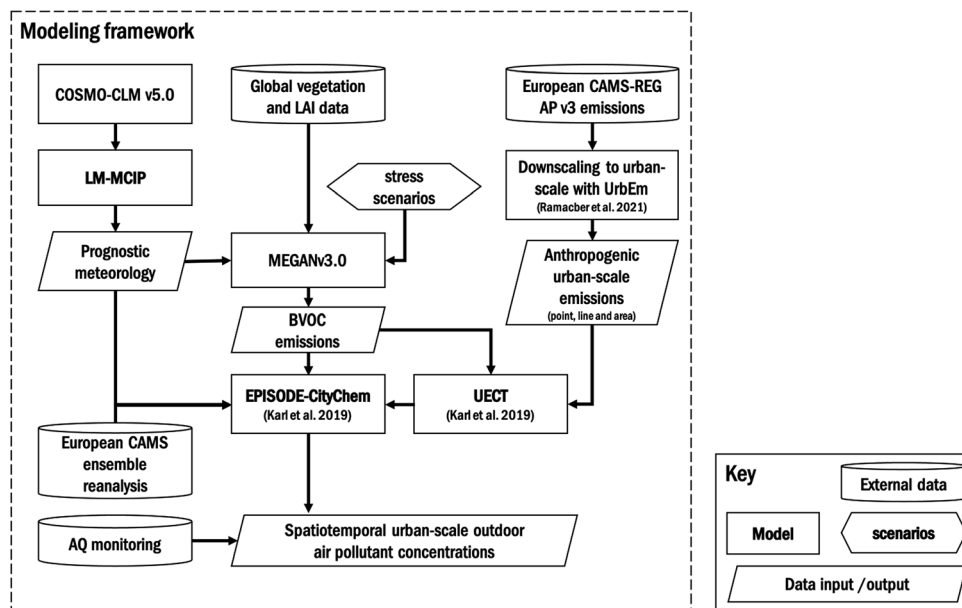
© 2022 The Author(s). Published by the Royal Society of Chemistry

Environ. Sci.: Atmos., 2022, **2**, 1132–1151 | **1135**

Fig. 1 Modeling framework to derive urban-scale pollutant concentrations, applying different stress scenarios for biogenic emissions.

and Paris that hold a share of GUA in the same order of magnitude. The European Environmental Agency (EEA) developed a city typology based on UGI to provide insight into the environmental performance of cities. This typology has been based on a cluster analysis that identifies cities with similar characteristics into one of the nine clusters. Hamburg belongs to the green sealed cities cluster. Main characteristics of this cluster are high sealing degrees, medium shares of GUA and low shares of urban forest. Alongside Hamburg there are mainly the large northern European cities such as Edinburgh, Dublin, Copenhagen, Stockholm and Helsinki in this category.[62] Accordingly, Hamburg exhibits conditions for urban BVOC research that can, to a certain extent, be considered representative for northern European cities except for Stockholm and Helsinki. Here the surrounding vegetation is dominated by forests (*e.g.*, *Picea abies*, *Pinus sylvestris* and *Betula pubescens*;[63]), while the main land use for Hamburg's surrounding is non-irrigated arable land (Fig. S7-1, 2†). Therefore, higher BVOC concentrations and different compositions are expected for Helsinki and Stockholm compared to Hamburg. The surrounding of Hamburg also shows contributions of other land use classes (see Fig. S7-1†). In the north-west pastures and in the south coniferous together with mixed forest dominate. Broad-leaved forests occur all around but with highest contribution east of Hamburg. Most common tree species are pine (*Pinus sylvestris*), spruce (*Picea abies*), Douglas fir (*Pseudotsuga menziesii*), beech (*Fags sylvatica*), oak (*Quercus robur*) and birch (*Betula pubescens*).

Within the city of Hamburg the most common tree species is *Quercus robur* and together with *Tilia spp.*, *Platanus spp.*, *Betula spp.*, *Acer spp.* and *Fraxinus spp.* represent two thirds of Hamburg's city trees.[61] *Quercus robur* is known to be a strong isoprene emitter,[11,64,65] a medium-to-low monoterpene and a low sesquiterpene emitter.[47]

Below, the models MEGAN3 and EPISODE-CityChem as well as their inputs for the calculations of BVOC emissions in the Hamburg metropolitan area and for the calculations of ozone concentrations in the city of Hamburg are described. The two different model domains are illustrated in Fig. 2.
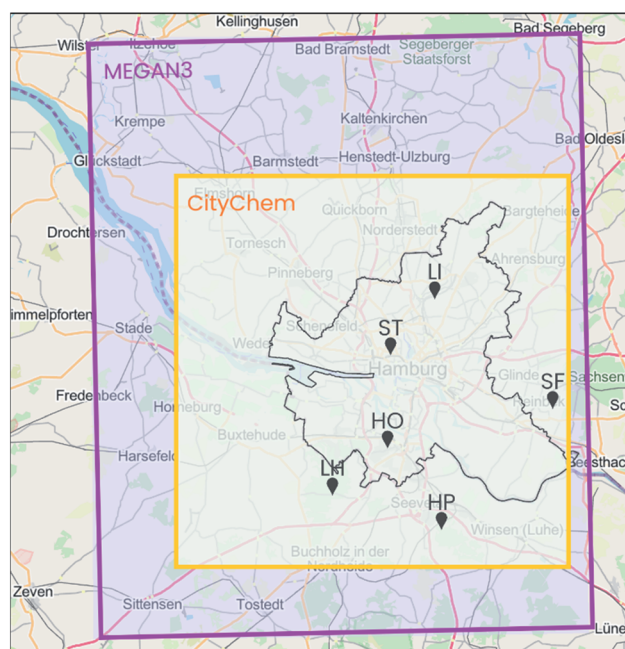

Fig. 2 Model domains of MEGAN3 and EPISODE-CityChem runs in WGS 84/UTM zone 32N projection. Stations: LH = Lüneburg Heath, HO = High impact ozone, SF = Sachsenwald Forest, ST = Stern-schanze, LI = Low impact isoprene, HP = High impact MPAN. Background map data © OpenStreetMap contributors, Microsoft, Facebook Inc. and its affiliates; Esri Community Maps, Map layer by Esri.

Table 1 Stress effects of different stress mechanisms in MEGAN3 on selected BVOC species and their total emissions in the growing period 2018 without stress effects. For entries marked with '−', no effect was found

BVOC Species	CO_2	Wind	Heat	Cold	Drought	Total stress	MEGANv3 domain without stress [t]
Isoprene	—	—	—	—	−65.3%	−65.3%	8032
APIN[a]	—	+0.7%	—	+0.3%	−55.5%	−54.8%	654
LIM[a]	—	+0.6%	—	+9.2%	−57.8%	−49.0%	77
Methanol	—	—	—	—	−58.1%	−58.1%	1218
Ethanol	—	+0.02%	—	+0.4%	−62.4%	−62.1%	150
Sesquiterpenes[b]	—	+0.7%	—	+6.3%	−65.9%	−60.0%	116
C_2H_6	—	—	—	—	−56.9%	−56.9%	38
HCHO	—	—	—	—	−56.9%	−56.9%	14
CH_3CHO	—	+0.1%	—	+0.7%	−62.2%	−61.6%	158
C_2H_4	—	—	—	—	−56.9%	−56.9%	67
nC_4H_{10}	—	—	—	—	−56.9%	−56.9%	46
$CH_3COC_2H_5$	—	+0.02%	—	+0.2%	−57.2%	−57.0%	127
C_3H_6	—	—	—	—	−58.0%	−58.0%	109

[a] Multiple species, which can be assigned to monoterpene group (following Table S2-3 in ESI S2). [b] Not taken into account in Emchem09-HET of EPISODE-CityChem v1.5.

3.2 MEGAN V3.0 description and setup

The Model of Emissions of Gases and Aerosols from Nature (MEGAN) is a high-resolution modelling system that estimates the net emissions from terrestrial ecosystems to the atmosphere.[23] For the presented study we applied MEGAN3 ref. 23,38,39 to calculate BVOC emissions under different stress and non-stress conditions. MEGAN is a global gridded emission model with a horizontal grid resolution of 1 km.[66] It calculates over 200 chemical compounds of biogenic origin, applying meteorological and soil parameters as well as vegetation and land use databases. Even though MEGAN was developed for global application, its calibration with regard to land use and plant types fits best for the US.

Compared with the former Version MEGAN v2.1 ref. 23 there are three major updates in MEGAN3. Firstly, the canopy environment model has been updated to improve the representation of canopy processes.

Now the model uses leaf temperature instead of air temperature to account for leaf energy balance, as well as procedures to consider canopy transparency and varying emission capacity as a function of canopy depth. Secondly, MEGAN3 introduces the MEGAN Emission Factor Processor (MEGAN-EFP) to provide suitable emission factor data. Finally, the emission activity response has been improved by the incorporation of stress response mechanisms. Regarding the emissions from canopy top, Guenther *et al.*[38] observed that isoprene emission generated with MEGAN3 were considerably lower than those from MEGAN v2.1 and thereby in much better agreement with canopy flux and concentration measurements.

3.2.1 Stress response mechanisms in MEGAN3.
There are several compound specific stress response mechanisms implemented in MEGAN3, which are triggered by different threshold mechanisms for drought conditions, extreme heat, cold and wind events, as well as at high concentrations of CO_2 and O_3.

Temperatures within a range of 20 °C to 30 °C are considered to be non-stressful for plants while temperatures below 10 °C or above 40 °C are considered stressful and thus expected to intensify or induce BVOC emissions. Consequently, temperatures between 10 °C and 20 °C exhibit a transition zone. When the temperature exceeds 40 °C, MEGAN3 applies a heat stress response. Therefore, emissions increase by a factor of five has been implemented for four stress VOC categories including monoterpenes and sesquiterpenes.

In this study, we will mainly focus on the impact of drought stress mechanisms due to the severe drought conditions in Europe in 2018.[41] Moreover, other stress mechanisms were barely triggered during the selected growing period in 2018 (Table 1). In MEGAN3, drought impacts on isoprene emission is taken into account by considering photosynthesis and water stress simultaneously.[67] A detailed summary of the stress mechanisms in MEGAN3 can be found in.[67]

3.2.2 MEGAN3 – setup.
In the MEGAN3 simulations, a 77 × 77 km² grid with 1 × 1 km² resolution was applied to the study domain (Fig. 2). The model is set up for the year 2018. The meteorological input data was taken from the coastDat3 dataset that was created with the Consortium for Small Scale Modelling Climate Limited-area Model (COSMO-CLM) Version 5.0.[55] The data has a spatial resolution of 0.11° × 0.11°. For further use, the data was fit to the model domain and downscaled to 1 × 1 km² spatial resolution using the Local Model Meteorology-Chemistry Interface Preprocessor (LM-MCIP). Further required model input for MEGAN3 includes global data tables containing information of crop, grass, shrubbery, deciduous, coniferous and tropical tree coverage. These data tables were downloaded from the MEGAN website (https://bai.ess.uci.edu/megan/data-and-code, last accessed on January 07 2022) and not modified for this study. Additionally, the SPOT/PROBA V LAI1 ref. 68,69 leaf area index (LAI) data was used as alternative input data for MEGAN3. It has a spatial resolution of 1 × 1 km² and a temporal resolution of 10 days.

© 2022 The Author(s). Published by the Royal Society of Chemistry

Environ. Sci.: Atmos., 2022, **2**, 1132–1151 | **1137**

3.3 EPISODE-CityChem – description & setup

EPISODE-CityChem[40] is an urban dispersion model, which simulates the photochemical transformation and atmospheric diffusion of multiple reactive pollutants in order to create pollutant concentration fields on a horizontal resolution of 100 m or finer on the urban scale. The City-scale Chemistry (CityChem) model, developed at Helmholtz-Zentrum Hereon, is an extension to the Eulerian model EPISODE[70] which was developed at the Norwegian Institute for Air Research (NILU) for air quality studies at the local scale. The primary focus of EPISODE-CityChem is on the simulation of urban ozone concentrations.

3.3.1 **EPISODE-CityChem – setup.** For the modelling of pollutant concentrations in Hamburg, we set up EPISODE-CityChem with a Eulerian main grid of 50×50 grid cells of 1×1 km^2 each and a Gaussian receptor grid of 500×500 grid cells of 100×100 m^2 each (Fig. 2). The vertical grid size varies from a few meters near the ground to several hundred meters at higher altitude, with a total height of up to 3759 m above ground.

The meteorological input data applied in the EPISODE-CityChem setup follows the meteorological datasets for 2018 that are used in the MEGAN3 setup as described above. To account for background pollutant concentrations, we applied hourly Copernicus Atmospheric Monitoring Services (CAMS) ensemble reanalysis for the year 2018. Emission data for anthropogenic land-based emission sectors is achieved from the regional CAMS emission inventory (CAMS-REG-AP), which was downscaled with a hybrid method to derive high-resolution emissions for the urban-scale (UrbEm;[71]). To achieve annual emissions for the shipping sector, a ship emission modeling system[72] was applied for the year 2018. For a detailed description of the applied anthropogenic emission inventory, we refer to ESI S1.†

3.3.2 **EPISODE-CityChem – implementation of BVOC emissions.** BVOC emissions are included as ozone precursors in the photochemical setup of EPISODE-CityChem for Hamburg 2018 and incorporated in the urban chemistry scheme EmChem09-HET. The urban chemistry scheme EmChem09-HET includes reactions between organic peroxy radicals and HO$_2$ radical as well as other organic peroxy radicals. It is appropriate for conditions ranging from highly polluted areas to low-NO$_x$ conditions in rural areas of the city domain.[40] With EmChem09-HET, the chemistry of isoprene and monoterpenes (represented as APIN and LIM) emitted by the urban vegetation can be simulated. The photo-oxidation of isoprene has been completely revised compared to the original EmChem09 mechanism presented in.[40] The revised isoprene reaction scheme is based on a modified version of the Mainz Isoprene Mechanism[73] published by Karl et al.[74] Two monoterpene groups, APIN and LIM are model surrogates to represent slower- and faster-reacting monoterpenes, respectively. EmChem09-HET considers the photo-oxidation of isoprene, APIN and LIM by the atmospheric oxidants OH, NO$_3$ and O$_3$. The reaction scheme of APIN is adopted from Bergström et al.[75] The reaction scheme of LIM is based on Calvert et al.[76]

In total, EmChem09-HET includes 78 chemical reactions and 28 photo-dissociation reactions. The chemical pre-processor GenChem[77] has been used to convert lists of input chemical species and reactions to differential equations. ESI Table S2-2† lists the chemical reactions of isoprene, APIN and LIM in EmChem09-HET.

With the EmChem09-HET reaction mechanism, it is now possible to consider several BVOC species as modelled with MEGAN3. In MEGAN there are in total 143 BVOC species, carbon monoxide (CO) and NO modelled as plant related emissions (Table S2-3†). For the emission input in the EPISODE-CityChem model we take into account 77 species, including isoprene, two monoterpene groups (APIN and LIM), methanol, ethanol, ethane (C$_2$H$_6$), formaldehyde (HCHO), acetaldehyde and higher aldehydes (CH$_3$CHO), ethene (C$_2$H$_4$), n-butane and other alkanes with $n > 3$ (nC$_4$H$_{10}$), methyl ethyl ketone and other ketones (CH$_3$COC$_2$H$_5$) and propene and other alkenes with $n > 4$ (C$_3$H$_6$) (Table S2-1 in ESI S2†). We did not take into account the MEGAN3 emissions of CO and soil emissions of NO in the urban simulations. Furthermore, 44 species that are classified as sesquiterpenes were not included in the simulations because currently sesquiterpenes are not included in the EmChem09-HET mechanism. All other individual BVOC chemical species from MEGAN3 were mapped to groups of species for the use in EPISODE-CityChem. Among others, the different individual monoterpene species were grouped in APIN (α-pinene, β-pinene, 3-carene, cymene and other relatively slow reacting monoterpenes) and LIM (limonene, myrcene, sabinene, ocimene and other fast reacting monoterpenes).[53] For a full mapping table, we refer to the ESI Table S2-3.†

After this classification, there are in total 12 species or groups of MEGAN3 emission species left that are prepared for the urban simulations. We differentiate these emissions in two groups: (1) BVOC emissions that are solely from biogenic sources, and (2) other volatile organic compound (VOC) emissions from biogenic sources in MEGAN for which there are also anthropogenic sources in the emission inventory for the CityChem domain. The first group consists of biogenic isoprene, APIN, LIM, methanol and ethanol. The MEGAN3 emission output for the first group was directly converted to hourly emissions for the CityChem model domain. The second group consists of C$_2$H$_6$, HCHO, CH$_3$CHO, C$_2$H$_4$, nC$_4$H$_{10}$, CH$_3$COC$_2$H$_5$, and C$_3$H$_6$ and was prepared as emission input to EPISODE-CityChem using the pre-processor UECT. This was done to combine the anthropogenic non-methane volatile organic compound (NMVOC) emissions from all urban emission sectors (such as solvent use) with the MEGAN biogenic emissions. Nevertheless, it was necessary to use annual emission totals for the second group to be processed in UECT. The temporal distribution of the second group is determined by the time profiles of the respective emission sector, not following the temporal distribution of MEGAN3 modeling, therefore, the second group should be considered as indirectly converted emission input.

Although we took into account multiple biogenic emission species from MEGAN3, this study focuses on the impact of isoprene emissions under different stress scenarios. Therefore,

1138 | Environ. Sci.: Atmos., 2022, **2**, 1132–1151

© 2022 The Author(s). Published by the Royal Society of Chemistry

we only considered boundary conditions for isoprene and peroxymethacryloyl nitrate (MPAN), a PAN-like primary reaction product from isoprene photo-oxidation. The boundary conditions for isoprene are taken into account as 3.8% of total NMVOC concentrations in the CAMS ensemble reanalysis at the boundaries of the CityChem domain, based on the typical NMVOC composition in Europe following Zimmermann & Poppe.[78] There is no distinction between anthropogenic and biogenic sources in the boundary conditions for isoprene. For other BVOC species, we did not consider boundary conditions.

4 Results

4.1 BVOC emissions calculated by MEGAN3

The scenarios simulated with MEGAN3 show the same trend for all simulated BVOC species under the environmental conditions of 2018. Table 1 summarizes the results of stress responses during the growing season 2018 (April until October).

Drought stress has the most significant impact for all species and manifests in decreasing BVOC emissions ranging from −49% for the group of LIM to −65% for isoprene. Besides drought stress, cold stress and wind stress are leading to a change in BVOC emissions, but only for the group of APIN, LIM, and sesquiterpenes, as well as for ethanol, CH_3CHO and $CH_3COC_2H_5$. For both wind and cold stress, emissions increase under stress conditions. While for the groups of LIM (+9%) and sesquiterpenes (+6%) there is a significant increase modelled under cold stress conditions, for the group of APIN, ethanol, CH_3CHO and $CH_3COC_2H_5$ the increase is below 1%. The effect of wind stress is similar for all species affected by wind stress. Stress responses concerning CO_2 and heat are not evident for any BVOC species.

The total emissions in the growing period are highest for isoprene with 8032 t isoprene in the MEGAN3 domain. Additionally, isoprene shows the strongest response to simulated

Table 2 Statistical evaluation of modelled maximum daily 8 hours rolling mean (MDA8) O_3 concentrations in August 2018 and the scenarios base, drought and noBVOC under application of four available O_3 measurement sites in the study domain ($n = 31$ for each site and scenario, a description of statistical parameters can be found in ESI S6)

Site	Scenario	FAC2	MB	NMB	RMSE	r
13ST	Base	0.968	−24.670	−0.287	32.373	0.454
13ST	Drought	0.968	−10.744	−0.288	32.453	0.453
13ST	noBVOC	0.968	−10.777	−0.288	32.483	0.453
24FL	Base	1.000	−0.111	−0.001	16.359	0.717
24FL	Drought	1.000	−0.139	−0.002	16.381	0.716
24FL	noBVOC	1.000	−0.197	−0.002	16.418	0.716
51BF	Base	0.968	−16.391	−0.181	−23.503	0.648
51BF	Drought	0.968	−16.397	−0.181	−23.512	0.647
51BF	noBVOC	0.968	−16.424	−0.181	−23.543	0.647
52NG	Base	1.000	−12.739	−0.134	−27.663	0.527
52NG	Drought	1.000	−12.785	−0.135	−27.713	0.526
52NG	noBVOC	1.000	−12.808	−0.135	−27.725	0.526

drought stress. The impact of stress mechanisms on isoprene emission is visualized in Fig. 3.

Isoprene is only responding to the drought stress mechanisms. The monthly isoprene emissions for the scenarios with heat and without stress mechanisms are illustrated in Fig. 3 as an average rate per km² for the MEGAN3 domain. First, it becomes evident, that there are barely emissions at the beginning and end of the growing period in 2018. Second, the impact of drought stress is highest in summer months (JJA), leading to decreased isoprene emissions by 84% in July.

4.2 Simulated concentrations from EPISODE-CityChem

The following chapter shows the results of all analysis focusing on isoprene and its reaction product concentrations including ozone from the simulations with EPISODE-CityChem. The modelled ozone concentrations were compared against available measurements in the study domain for different scenarios; a statistical evaluation can be found in ESI Table S3-1 for O_3, S4-1 for NO_2 and ESI S5 for meteorological parameters.† A detailed description of the applied statistical indicators can be found in ESI S6.† Here, we present a condensed evaluation of O_3 in August at available measurement sites in Table 2.

4.2.1 Isoprene. We present results from the EPISODE-CityChem simulations for the inner, Hamburg, domain (short: CityChem domain). Three simulations were performed for the growing season in 2018: (1) a scenario run including BVOC emissions under non-stressful conditions (base), (2) a scenario run including BVOC emissions under drought stress (drought), and (3) a scenario run without BVOC emissions (noBVOC). Fig. 4a shows the isoprene concentration distribution in the CityChem domain for July 2018 without stress application (base). Peaks in isoprene concentrations match with green areas in the domain, such as the Lüneburg Heath (LH) or the Sachsenwald Forest (SF). Fig. 4b shows the percentage change between isoprene concentrations calculated with isoprene emissions under stress application and isoprene emissions without stress application in the study area.

Fig. 3 Monthly isoprene emission rates of the base (blue) and drought (yellow) scenario averaged for the MEGAN domain [kg km⁻¹²]. The percentage values show the monthly relative reduction in emission rates of the drought scenario compared to the base scenario.
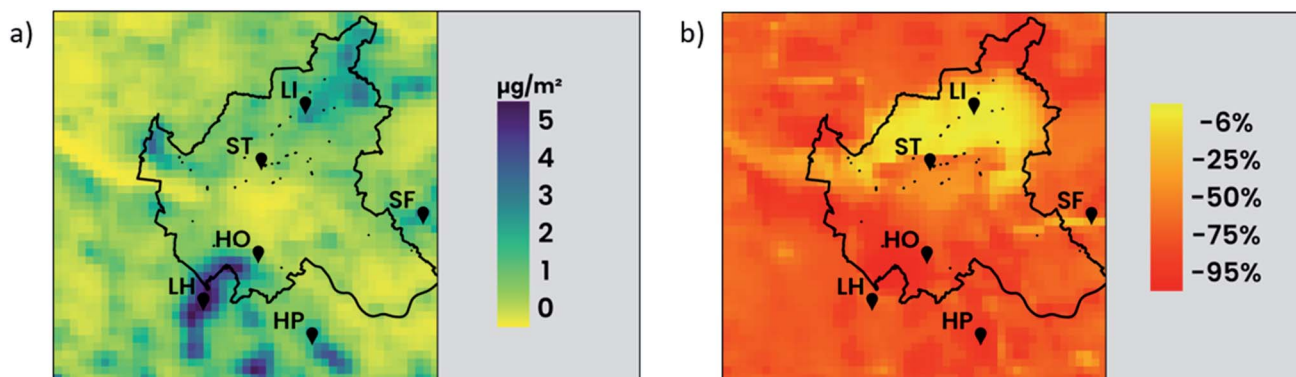
Fig. 4 Isoprene concentration distribution in the EPISODE-CityChem domain for July 2018 and the effect of drought stress. (4a) illustrates the modeled isoprene concentrations under non-stressful conditions (base case), (4b) depicts the relative reduction of isoprene concentrations due to drought stress (difference drought − base).

Fig. 5 Diurnal variations in mean isoprene concentrations by wind direction for all points of interest in July 2018 without stress application. Note that, isoprene concentrations do not only originate from local isoprene emissions in the study area. EPISODE-CityChem also calculates the atmospheric transport of isoprene from rural areas into the city, taking into account isoprene concentrations at the regional domain boundaries that are transported into th5e study area (Section 2.3.2).

It is detectable that the stress-impact reduces the isoprene concentrations in the entire study area. This reduction ranges between 6% and 95%. The highest impact is observable in the southern part of the city, in the LH area, and south of the Elbe River basin. In general, the reductions are smallest in the highly sealed city center, along the Elbe River, and in the port-area where the abundance of vegetation and thus BVOC emitters is smallest. To further investigate the isoprene chemistry in areas with a low stress-effect, a point within the area of the least impact on isoprene and relatively high isoprene concentrations was identified (LI). Additionally, HO and HP were selected as points of interest because they show a high impact on ozone and MPAN, respectively. Also, the monitoring station Stern-schanze (ST) has been chosen because it is an urban station which already depicted relatively high ozone concentrations in former studies.[40,44]

4.2.2 Pollution roses. We analyzed the dependencies of isoprene concentrations on wind speed and wind direction at several locations inside the CityChem domain, and display them as pollution roses in Fig. 5 and 6. In this analysis, the period of 24–26. July has been excluded, during which night-time peaks in NMVOC boundary conditions occurred, which obscure the local isoprene concentrations. This transport from the boundaries erroneously indicated very high isoprene concentrations for strong winds (6–8 m s^{-1}) from northern directions at all stations.

Fig. 5 illustrates the mean isoprene concentrations as pollution roses for all points of interest. LH shows the highest mean values with a maximum at 2–4 m s^{-1} wind speed from southwestern directions. Moreover, concentrations tend to be relatively high for southerly and southwesterly winds at all points of interest indicating an influence from the southern

Fig. 6 Mean concentrations of isoprene in wind speed/direction bins for all points of interest in July 2018 without stress application (base case). Pollution wind roses show increments of 2 m s^{-1} in axial direction from 0 m s^{-1} in the center to 10 m s^{-1}. Calm winds were included, but make up for less than 0.5% of the winds from each direction.

Fig. 7 Modelled hourly concentrations of Isoprene, MACR and MPAN at point HP: (a) for the base scenario (7a) and (b) for the drought scenario (7b). The highlighted area marks the dry period July 25 to July 31, 2018.

Fig. 8 Normalized mean diurnal variations for MACR, MPAN, isoprene, ozone, NO and NO_2 in July for different scenarios at HP. Time in hours on the x-axis refers to local time.

part of the CityChem domain, which would be in agreement with isoprene emissions from the surrounding vegetation areas, mainly from forest areas south of Hamburg. The locations LH, LI and HP in the southern part of the domain show the highest isoprene concentrations on average.

Fig. 6 illustrates the diurnal variations of mean isoprene concentrations in relation to wind direction. Again, LH depicts highest overall values. This figure shows that there is no isoprene production at nighttime, since isoprene is a byproduct of photosynthesis, and rapidly removed from the air by reaction with atmospheric oxidants. Moreover, the diurnal variation reveals two periods when concentrations are pronounced at all points of interest and especially in situations with wind from southwesterly and easterly directions. The first period lies in the morning between seven and 8 am (local time, LT) and marks the onset of local isoprene production. The second period matches the end of daily isoprene production between six and 8 pm LT. While isoprene emissions peak at noon, the relatively fast reaction with the atmospheric OH radicals depletes isoprene concentrations during the sunlit daytime.

The directional distribution of mean isoprene concentrations found in the pollution roses (Fig. 5) is largely reproduced. In general, distributing the concentrations by time and wind direction instead of wind speed and direction led to slightly smaller mean concentrations due to averaging over hours with different wind speed. The diurnal variation of isoprene will be further explored in the next section.

4.2.3   Isoprene and its oxidation products. Fig. 7 shows the time series for concentrations of isoprene and its oxidation products, methacrolein (MACR) and MPAN in July 2018 at the point of highest MPAN impact (HP). The highlighted area marks the dry period that was identified in that month. Both MACR and MPAN are formed when isoprene is oxidized which affects ozone formation processes. As the production of MACR is often

linked to NO, which impacts NO to NO_2 conversion and consequently ozone formation, their concentration levels can reveal information about temporal ozone formation patterns from isoprene with and without drought stress. In Fig. 7a, the temporal pattern of MACR follows the one of isoprene with a recurring drop at nighttime. Both compounds show a strong peak with beginning drought, but MACR stays low while isoprene returns to a level which is higher (+38%) than before the dry period. Since Fig. 7a depicts the time series without stress application, the high isoprene peaks are very likely explained by increased temperatures during that period. The temporal variations in MPAN reveal an opposing trend to isoprene and MACR with lowest concentrations during midday and elevated concentrations in the morning and evening. As MPAN is a second-generation oxidation product of MACR and linked to NO_2 (IS-21) the local production of MPAN is partly coupled to NO_2 emission peaks.

Fig. 7b shows the time series of concentrations for isoprene, MACR and MPAN under drought conditions. The mean concentrations for all compounds were reduced by drought stress, but less for MPAN (−20%) than for isoprene and MACR (approximately −80%). The temporal patterns do not differ significantly from the base scenario. The diurnal variations of isoprene, MACR and MPAN will be further explored in the next paragraph.

4.2.4   Diurnal variations. Fig. 8 shows the averaged diurnal cycle for MACR, MPAN, isoprene, ozone, NO and NO_2 normalized by their mean values in July for different scenarios at the point of highest ozone impact (HO). The diurnal variations of the normalized ozone, NO and NO_2 concentrations do not show any significant changes between the different scenarios at HP. The noBVOC scenario shows the smallest normalized concentrations for MACR and isoprene. The drought scenario includes the BVOC emissions from MEGAN3 calculated by applying the

1142 | *Environ. Sci.: Atmos.*, 2022, **2**, 1132–1151

© 2022 The Author(s). Published by the Royal Society of Chemistry

drought stress mechanisms. Both isoprene and MACR are elevated compared to the noBVOC scenario. Lastly, the base scenario depicts the concentrations that were derived from calculations with BVOC emissions under no-stress conditions. Here, isoprene and MACR concentrations are highest and show clear trends. Isoprene emission is coupled to photosynthesis; therefore, emissions increase in the morning after sunrise until the photochemical production of ozone and OH radicals become sufficient and a balance between isoprene degradation and the local emissions is reached. When ozone and OH formation is not sufficient anymore isoprene concentration increases again until synthesis emission ceases and progressing degradation reduces isoprene concentrations. As MACR and MPAN are reaction products of isoprene its daily cycle is linked to isoprene concentration, their concentrations show a clear daytime component but with two peaks during the day linked to traffic emissions. MACR has one pronounced peak around 9–10 am LT just after NO peaks. Afterwards the concentration declines until a smaller second peak at around 4 pm is reached, again linked to NO. Thereafter MACR concentration further declines until around 8 pm in the evening, when its concentration reaches background concentration levels. The production of MPAN follows the daily course of NO_2 that exhibits peaks during the traffic rush hour times in the morning (6–9 am) and late afternoon (5–7 pm LT). Due to its persistence in the atmosphere, MPAN is advected from the regional background into the city (Section 2.3.2). The atmospheric persistence of MPAN, like for other peroxyacyl nitrates, is limited by their

thermal decomposition, which increases rapidly as temperature increases.[79] MPAN can be transported further downwind from the area where it was produced and if transported down to the surface, it can thermally decompose to regenerate NO_x in areas with less direct anthropogenic production of NO_x, where the regenerated NO_x can enhance ozone production. However, MPAN can be removed by the OH radical much faster than PAN, which reduces its importance as reservoir for long-range transport of reactive nitrogen, compared to PAN.

4.2.5 Isoprene – ozone interaction under influence of drought stress. To assess how drought stress affects the modelled spatial distribution and transport of isoprene and ozone, two diagonal transects were created for the CityChem domain. Both transects only consider concentrations from daylight hours (6 am to 6 pm) because there is no isoprene formation during nighttime. The pathways of both transects are displayed in Fig. 9a–b and 10a and b.

The first transects connects the northwestern corner of the domain to the southeastern corner. This transect has been timed to cover a dry period in July (July 25 to July 31) in order to illustrate the highest possible changes in both isoprene and ozone concentrations due to drought stress. Winds from NW with an average wind speed of 2 m s⁻¹ dominated this period, therefore, this transect is suitable to account for the atmospheric transport of compounds besides their local formation. Fig. 9c displays the differences in ozone and isoprene concentrations due to drought stress along the NW-SE transect during the dry period. The background shading indicates different
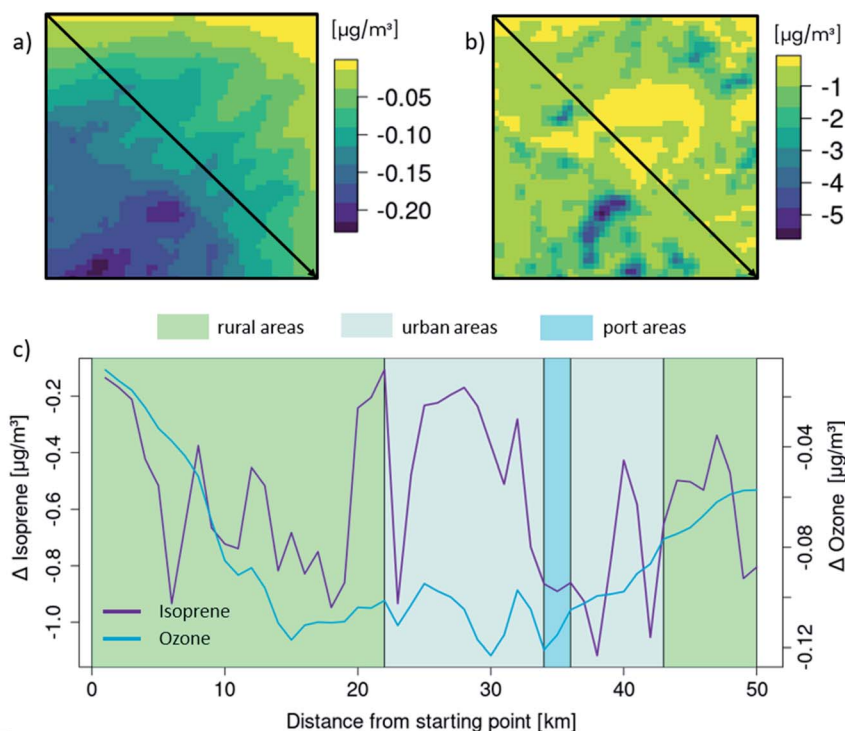

Fig. 9 Absolute differences in ozone concentrations (9a) and isoprene concentrations (9b) due to drought stress in July 2018 and diagonal transect (NW-SE) of differences in ozone and isoprene concentrations (9c) due to drought stress throughout the study domain for a dry period in July 2018.

© 2022 The Author(s). Published by the Royal Society of Chemistry

Environ. Sci.: Atmos., 2022, **2**, 1132–1151 | **1143**

types of land use. The transect reveals similar patterns for the changes in isoprene and ozone concentrations, even though their intensity differs by a factor of 10. Reduction of isoprene concentrations due to drought stress spatially coincide with reduction of ozone concentrations. This response in ozone appears to have a minor delay to changes in isoprene levels. The ozone reduction is highest in the central urban areas. Note that changes in isoprene and ozone are not necessarily expected to be spatially related. The atmospheric lifetime of isoprene due to daytime OH radical concentration is typically about 1 hour, so the ozone response to isoprene decrease might be decoupled from the place of emission. At wind speed of 2 m s^{-1}, the air parcel could travel 7.2 km in one hour. However, the drought effect seems to affect isoprene and ozone homogeneously throughout the domain and the extent of the domain is large enough to unveil the response of ozone to reduced isoprene production along the transect.

The second transect passes from the southwestern corner to the northeastern corner of the domain. This transect has been timed to match a period with dominant winds from SW directions (June 14 – June 20, avg. wind speed = 2 m s^{-1}) which may transport isoprene into the study domain and resulting in higher isoprene concentrations (Fig. 5). For this period, the changes in isoprene exceeds the changes in ozone almost by a factor of 20. Similar to the first transect, there is a detectable response of ozone to isoprene levels. However, this response is not as pronounced as for the first transect. This might be explained by the fact that the first transect was timed for a dry

period with an expectably high impact of the modelled drought stress. However, the isoprene differences due to drought stress are not much smaller than in the first transect. The lower photochemical activity in June and higher wind speeds are probably the reason why O$_3$ is less affected: modelled average daytime OH concentration during the June drought period (∼4 × 106 molecules/cm^3) was lower than during the drought period in July (∼7 × 10^6 molecules/cm^3).

4.2.6 Photochemical production of ozone. To assess the impact of stress-affected isoprene emissions on surface ozone concentrations, the percentage change in monthly mean ozone concentrations (July 2018) due to drought stress is illustrated in Fig. 11.

The relative change between ozone concentrations is calculated by comparing the scenarios with isoprene emissions under stress (drought) and no-stress applications (base) within the study area. Accordingly, it depicts the impact of stress-affected isoprene emissions on ozone concentrations. It is detectable that the stress-impact reduces the ozone concentrations in the entire study area. This reduction ranges between 0.01% and 0.15%. The highest impact is observable in the south and south-east of the study area. Since the ozone formation rate is controlled by photochemical reaction cycles involving VOCs and NO$_x$, it is plausible that ozone concentrations are lower if isoprene emissions are suppressed by stress in high NO$_x$ environments like Hamburg.

Under conditions with no stress, isoprene emissions are higher, potentially leading to higher O$_3$ concentrations.

Fig. 10 Absolute differences in ozone concentrations (10a) and isoprene concentrations (10b) due to drought stress in July 2018 and diagonal transect (SW-NE) of differences in ozone and isoprene concentrations (10c) due to drought stress throughout the study domain for a dry period in July 2018.

1144 | *Environ. Sci.: Atmos.*, 2022, **2**, 1132–1151

© 2022 The Author(s). Published by the Royal Society of Chemistry

Fig. 11 Monthly mean ozone concentrations in the EPISODE-CityChem domain for July 2018 and the effect of drought stress. (11a) ozone concentrations without drought stress; (11b) the relative reduction of ozone concentrations due to drought stress.

Compared to the noBVOC scenario (not shown) ozone concentrations in the base case (using local isoprene emissions) increased over the whole domain by up to 0.05 µg m^{-3} for maximum and 0.07 µg m^{-3} for mean values during the studied time period. This corresponds to a contribution of isoprene emissions to near-ground O_3 concentrations of 0.1% on domain average. Hence, the impact of isoprene emissions on urban ozone concentrations in Hamburg is small.

Based on a large field data set on isoprene and isoprene oxidation product concentrations in North America, Barket et al.[80] concluded a substantial increase in ozone production from isoprene between 0.1 ppb and 10 ppb (ca. 0.2–19 µg m^{-3}) of NO_x, whereas O_3 production from isoprene begins to decrease at sufficiently high NO_x concentrations (>~40 µg m^{-3}). In Hamburg, monthly NO_x concentrations are in the range 5–35 µg m^{-3}, covering the range that should favor ozone production from isoprene. While the findings of Barket et al.[80] suggest that anthropogenic NO_x sources can boost isoprene oxidation, only a weak influence of isoprene on O_3 production is found in our study.

The chemical regime, i.e., NO_x-limited or VOC-limited, defines what happens if VOC emissions are changed. In a NO_x-limited regime, an increase or reduction in BVOC emissions does not significantly affect ozone formation, while an increase in NO_x under constant BVOC conditions triggers a rapid ozone increase. In a VOC limited regime, sufficient NO_x is available but BVOCs are limited. Here, an increase in BVOC emissions under constant NO_x conditions can increase ozone.

The modelled VOC/NO_x ratio (ppmC/ppm) on monthly average in July 2018 was <1.5 for most parts of Hamburg city. Only in the rural areas in the northeast and southwest, the ratio was higher, indicating that the airflow from forested areas to the inner city is governed by the VOC-limited regime, where O_3 can potentially increase with increasing VOC emissions. However, from northwestern directions (predominant inflow to Hamburg is from NW) only small quantities of isoprene are advected to the inner city (see Fig. 5). NO_x emissions are high in many parts of the city due to traffic and shipping activities in the port. The area in the Southeast of Hamburg has the highest sensitivity for ozone increase with increasing BVOC emissions, because in the outflow of the city, NO_x from inner-city sources is

mixed with fresh BVOC emissions from sub-urban areas and can amplify ozone formation.[44]

In view of the identified VOC-limited regime, it is likely that future reductions in NO_x emissions and/or increased BVOC emissions lead to an enhanced photochemical production of O_3 in Hamburg.

It is important to keep track of BVOC emissions regarding ozone formation since changes in species composition or the expansion of urban green can shift the VOC-limited regime towards a transition zone between VOC-limited and NO_x-limited regimes. These transition zones depict favorable conditions for additional photochemical ozone formation.[11]

5 Discussion

5.1 Stress effects on BVOC emissions

We compared the MEGAN3-calculated BVOC emissions in the Hamburg metropolitan region to BVOC emission data for Germany reported in the literature. Oderbolz et al.[32] reported BVOC emissions for a region that corresponds closest to the Hamburg area of approximately 0.4 t km^{-2} a^{-1} for isoprene, 0.6 t km^{-2} a^{-1} for monoterpenes and 0.1 t km^{-2} a^{-1} for sesquiterpenes. The emissions modelled with MEGAN3 are in the same order of magnitude. In our study area it appears consequential that isoprene contributes the largest part to the total BVOC emissions (see Fig. 12) since the most abundant tree species (Q. robur) in Hamburg is a strong isoprene emitter. Fig. 12 shows the compound mix for the base scenario (inner circle) and for the drought scenario (outer circle).

The strong relative contribution of isoprene emissions is noteworthy. The other relevant tree species, namely Tilia spp., Platanus spp., Betula spp., Acer spp. and Fraxinus spp., predominantly emit sesquiterpenes and oxygenated VOCs, notably, Platanus spp. is an isoprene emitter with low emission potential and small influence on ozone production.[12]

Drought stress induces a strong signal in BVOC emissions in Hamburg. This was expectable, since Hamburg has a high degree of sealing which makes it harder for precipitation to infiltrate the soil. In MEGAN3, this effect is represented by low soil moisture. During drought periods, soil moisture in the study domain was up to 70% lower compared to wet periods.
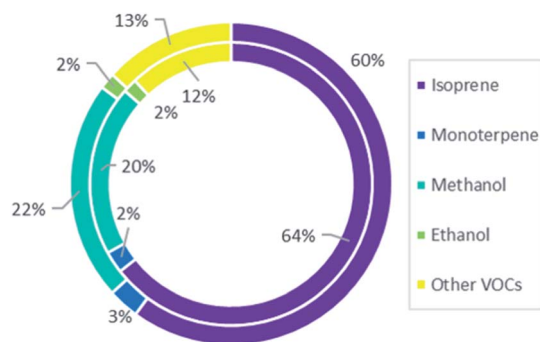
© 2022 The Author(s). Published by the Royal Society of Chemistry

Environ. Sci.: Atmos., 2022, **2**, 1132–1151 | **1145**

Fig. 12 Fraction of different compounds in total BVOC emissions in the MEGAN domain for the base scenario (inner circle) and drought scenario (outer circle).

The effect of drought stress on BVOC emissions spatially matches with green areas in the Hamburg metropolitan region. This phenomenon is most distinct for the SF and the northern LH areas. The drought stress response mechanism is applied by MEGAN3 when the soil moisture approaches the wilting point, below which plants cannot pull water out of the soil anymore.[81] With drought onset, plants are still able to maintain BVOC emissions as under drought conditions, isoprene production becomes uncoupled from photosynthesis by using alternative carbon sources such as starch breakdown to compensate the curtailed photosynthetic carbon input. However, under prolonged or heavy drought stress, all BVOC emissions are suppressed due to decreases in general plant performance.[28]

A comparable tendency was found by a study in Birmingham, England, which estimated BVOC emissions from urban trees, found that isoprene emissions from stressed trees were by a factor of 0.9 lower than those from unstressed trees.[82] Tree species that were examined in that study are *Q. robur* and *Betula spp*. However, the study defined stressful conditions simply as the exposure to an urban environment; in which drought or pollution frequently occur. That study can still serve as a good basis for comparisons with this study, since the environmental conditions for Birmingham are quite similar to those for Hamburg. Additionally, similar tree species were studied in both cities.

5.2 Effect of BVOC emissions on air quality

Isoprene photooxidation is a major driver of atmospheric chemistry in forested regions due to its highly reactive behavior with OH radicals, NO_3 radicals and ozone. Thus, changes in isoprene emissions are expected to affect ozone levels significantly.[81] The optimum for ozone formation lies in the transition zones between VOC-limited regimes (urban) and NO_x-limited regimes (rural). Thus, high BVOC emitters can create ideal ozone formation conditions within cities,[11] because their emissions alter the ratio of reactivity-weighted VOCs to NO_x and makes NO_x-limited regimes more likely with progressing air quality measures, *e.g.* NO_x emission reduction, in combination with climate mitigation measures, *e.g.* extending the UGI. The reaction between NO_x and BVOCs leads to maximization of

photochemical ozone formation especially under hot, dry, calm and light intense conditions such as heat waves.[11,83] According to urban-scale studies from China, BVOC emissions from urban green spaces play a vital role in modulating ozone formation[84] and have the potential to fill the gaps in models oftentimes underestimated ozone concentrations during high ozone episodes.[85]

A study in Berlin by Churkina *et al.*[33] found that BVOC emissions contribute substantially (∼12%) to the 8 h daily maximum concentrations of near-surface ozone in summer. Highest contributions were found in July, which correlates with high BVOC emissions rates due to high temperatures in that month. This contribution is highly elevated under heat wave conditions. During the heat wave in July 2006, the contribution of BVOC emissions to ozone concentrations in Berlin reached up to 60% on particular days.[33]

There are several explanations for the high contribution of isoprene to ozone formation in the simulation of Churkina *et al.*[33] compared to the rather low average impact of isoprene on O_3 in Hamburg found in the present study. Firstly, their study uses the first released version of MEGAN.[66] This version depicts large differences in the canopy environment model compared with MEGAN3. Most importantly, the version used by Churkina *et al.*[33] uses hourly averaged canopy air temperatures for the emission response algorithm, whereas MEGAN3 uses the leaf temperature, thereby accounting for leaf energy balance. A thorough comparison between different versions of MEGAN by Zhang *et al.* (2021)[86] revealed that the effect of BVOC emissions on ozone concentrations is highly sensitive towards the used version of MEGAN. Secondly, Churkina *et al.*[33] used a different land cover classification to adjust the MEGAN land cover data set to some extent,[33] whilst this study is based on alternative land use data. Luttkus *et al.*[21] found that the use of generalized land use classes instead of species-specific information could lead to an overestimation in BVOC emissions of up to 50% for Germany. Due to this overestimation, ozone concentrations tend to be elevated by 2.5% on average. Furthermore, Brandenburg (the region surrounding Berlin) mainly due its continental climate and high area fraction of pine trees is the region with highest BVOC emissions, as well as ozone and SOA concentrations in Germany – independent of the applied land use information.[21]

5.3 Potential relevance of other stresses

Various stressors that act on BVOC emissions can have opposing effects. Under climate change conditions or heat wave conditions in general, most of these abiotic stressors, but mainly heat and drought are expected to appear simultaneously. On the one hand, isoprene emissions are highly light and temperature dependent and increase with rising temperatures. On the other hand, severe drought reduces isoprene emission potentials.[87] The combined effect of both stressors should be further investigated in order to make assumptions about potential changes in BVOC emission patterns under future climate conditions.

BVOC emissions in urban environments do not only contribute to ozone formation, but can be affected by ozone

itself. Ozone exposes oxidative stress on plants, which can cause cell damage or inhibit the photosynthetic rate. Consequentially, ozone should on the one hand decrease constitutive BVOC emissions and induce emissions of compounds such as green leaf volatiles (GLVs), indicators for damage of cellular membranes. Still, BVOC responses to ozone stress are highly uncertain as reported results vary from study to study.[88–90] *Q. robur* trees that were exposed to ozone resulted in faster stomatal closure, partially mitigating drought stress effects.[91] For isoprene emissions it has been demonstrated that exposure to elevated ozone concentrations can both increase and decrease emission rates.[28]

6 Conclusions and outlook

We estimated the net impact of drought stress on isoprene and other BVOC emissions from vegetation in the urban area of Hamburg (DE) and its surrounding by applying the BVOC emission model MEGAN3 and the urban-scale CTM EPISODE-CityChem, updated to account for more BVOCs within the chemistry mechanism.

This paper provides relevant findings on the links between plant stress responses, BVOC emissions and urban ozone concentrations. To date, only few studies linked the alteration of BVOC emissions by environmental stressors with changes in urban ozone concentrations. Therefore, this work intends to contribute a further step towards a better understanding of the role of BVOC emissions in urban environments. To our knowledge, this is the first time that the MEGAN3 model was applied for an urban-scale CTM study. With the applied modeling chain including the additional developments made, it is possible to take into account the urban atmospheric chemistry including O_3 interactions with BVOCs emitted by natural sources within an urban area and its surrounding vegetation. Thus, the presented method allows *e.g.*, for evaluating UGI air pollutant abatement and climate mitigation strategies in urban areas in similar environments.

The accuracy of data on land use and plant types applied in the BVOC emission model is a crucial input for such a modelling experiment. In this study, we applied regional-scale land use data, which might lead to over- or underestimation of BVOC emissions and finally concentrations in the urban area of Hamburg.

Besides this limitation, we identified that BVOC emissions in Hamburg are influenced significantly by drought stress with 65% less isoprene emissions in the growing period 2018 compared to non-stress conditions. The highest stress impacts have been found for June, July and August for the surroundings of the city, especially in the South. The modelled reduction in isoprene concentrations ranges between 6% and 95%, again with the highest impact in the southern part of Hamburg's surroundings. In general, the reductions are smallest in the highly sealed city center.

The impact of isoprene on O_3 concentrations using local isoprene emissions as additional area source increased monthly mean ozone concentrations over the whole domain by up to 0.5 $\mu g\ m^{-3}$ (maximum) and 0.07 $\mu g\ m^{-3}$ (mean). Hence, the impact of isoprene emissions on absolute urban ozone concentrations

in Hamburg is small. Areas with expectably high BVOC emissions were included in the MEGAN3 domain, but not in the CTM domain. Therefore, potentially higher contributions to ozone formation in those areas, especially east of Hamburg have not been considered in this study.

Although the overall impact of isoprene on O_3 is currently rather small in the Hamburg area, this might change in the future. The modelled monthly mean VOC/NO_x ratio for July 2018 was smaller than 1.5 for most parts of the city. Thus, we identified a VOC-limited regime, and it is likely that future reductions in NO_x emissions and/or increased BVOC emissions lead to an enhanced photochemical production of O_3 in Hamburg, where biogenic emissions might play a more important role. Thus, it is important to consider BVOC emissions with respect to ozone formation if changes in tree species composition or extension of urban green are envisaged, since this might shift the VOC-limited regime to a transition zone between VOC-limited and NO_x-limited regimes.

Moreover, since isoprene emitters are suspected to be able to acclimate to past temperatures, an increase in isoprene emission potentials is expected for Hamburg, as the German Weather Service (DWD) reported an uninterrupted temperature rise in Hamburg since 1991 and a further increase of the temperature for the region is projected.[43] The area of Hamburg was chosen as an example for a city in northern Europe with predominant maritime influence, which in a changing climate is expected to face heat waves accompanied by droughts more frequently.[43] This expectation is further supported by the fact that isoprene production in plants under mild drought stress is decoupled from photosynthesis and thus more resistant towards reduced carbon availability in drought conditions.[28] If trees experience stresses such as heat or drought, the stomatal uptake of ozone is outweighed by BVOC production and thus ozone potentials increase rapidly.[10] The expected availability of studies addressing the issue of heat stress behavior for different plant and BVOC species near the *break point* between increase and decrease of BVOC emissions and their implementation into the model would allow for more dedicated assessments of the competing effects of emission increase during heat stress situations and emission decrease in concurrent drought phases. The currently implemented heat stress mechanism with a sole threshold of 40 °C was not activated for the Hamburg region even in the extreme summer of 2018.

Finally, the method and insights of this study in terms of a relation between BVOC emissions and O_3 concentrations in urban areas, which are comparable to the Hamburg urban area, will become more important with regard to future climate change and human health issues in urban environments.

Author contributions

Conceptualization: MOPR, JF, MQ, MK. Data curation: MOPR, JF. Formal Analysis: MOPR, JF. Investigation: MOPR, JF, MQ, MK. Methodology: MOPR, JF, MK. Software: MK. Supervision: MQ. Validation: JF. Visualization: MOPR, MLL, JF. Writing – original draft: JF. Writing – review & editing: MOPR, MLL, MQ; MK.

© 2022 The Author(s). Published by the Royal Society of Chemistry

Environ. Sci.: Atmos., 2022, **2**, 1132–1151 | **1147**

Conflicts of interest

There are no conflicts to declare.

Acknowledgements

Notes and references

1 IPCC, *Climate Change 2022: Impacts, Adaption, and Vulnerability. Contribution of Working Group II to the Sixth Assessment Report of the Intergovernmental Panel on Climate Change*, Cambridge, 2022.

2 EEA, *Europe's air quality status 2021- update*, https://www.eea.europa.eu/publications/air-quality-in-europe-2021/air-quality-status-briefing-2021, (accessed 1 April 2022).

3 J.-F. Bastin, Y. Finegold, C. Garcia, D. Mollicone, M. Rezende, D. Routh, C. M. Zohner and T. W. Crowther, The global tree restoration potential, *Science*, 2019, **365**, 76–79.

4 B. W. Griscom, J. Adams, P. W. Ellis, R. A. Houghton, G. Lomax, D. A. Miteva, W. H. Schlesinger, D. Shoch, J. V. Siikamäki, P. Smith, P. Woodbury, C. Zganjar, A. Blackman, J. Campari, R. T. Conant, C. Delgado, P. Elias, T. Gopalakrishna, M. R. Hamsik, M. Herrero, J. Kiesecker, E. Landis, L. Laestadius, S. M. Leavitt, S. Minnemeyer, S. Polasky, P. Potapov, F. E. Putz, J. Sanderman, M. Silvius, E. Wollenberg and J. Fargione, Natural climate solutions, *Proc. Natl. Acad. Sci. U. S. A.*, 2017, **114**, 11645–11650.

5 A. Arneth, S. P. Harrison, S. Zaehle, K. Tsigaridis, S. Menon, P. J. Bartlein, J. Feichter, A. Korhola, M. Kulmala, D. O'Donnell, G. Schurgers, S. Sorvari and T. Vesala, Terrestrial biogeochemical feedbacks in the climate system, *Nat. Geosci.*, 2010, **3**, 525–532.

6 S. Schubert and S. Grossman-Clarke, The Influence of green areas and roof albedos on air temperatures during Extreme Heat Events in Berlin, Germany, *metz*, 2013, **22**, 131–143.

7 EEA, Urban sustainability, in *Europe. What Is Driving Cities' Environmental Change?*, 2021.

8 Moser, *et al.*, City trees: Growth, functions and services, *Allg. Forst- Jagdztg.*, 2017, **188**, 94–111.

9 G. Popkin, How much can forests fight climate change?, *Nature*, 2019, **565**, 280–282.

10 T. S. Eisenman, G. Churkina, S. P. Jariwala, P. Kumar, G. S. Lovasi, D. E. Pataki, K. R. Weinberger and T. H. Whitlow, Urban trees, air quality, and asthma: An interdisciplinary review, *Landscape and Urban Planning*, 2019, **187**, 47–59.

11 C. Calfapietra, S. Fares, F. Manes, A. Morani, G. Sgrigna and F. Loreto, Role of Biogenic Volatile Organic Compounds (BVOC) emitted by urban trees on ozone concentration in cities: a review, *Environ. Pollut.*, 2013, **183**, 71–80.

12 A. C. Fitzky, H. Sandén, T. Karl, S. Fares, C. Calfapietra, R. Grote, A. Saunier and B. Rewald, The Interplay Between Ozone and Urban Vegetation—BVOC Emissions, Ozone Deposition, and Tree Ecophysiology, *Front. For. Glob. Change*, 2019, **2**, 403.

13 M. Brune, *Urban Trees under Climate Change*, 2016.

14 T. R. Oke, G. Mills, A. Christen and J. A. Voogt, *Urban Climates*, Cambridge University Press, Cambridge, 2017.

15 S. J. Livesley, G. M. McPherson and C. Calfapietra, The Urban Forest and Ecosystem Services: Impacts on Urban Water, Heat, and Pollution Cycles at the Tree, Street, and City Scale, *J. Environ. Qual.*, 2016, **45**, 119–124.

16 N. Kabisch, C. Püffel, O. Masztalerz, J. Hemmerling and R. Kraemer, Physiological and psychological effects of visits to different urban green and street environments in older people: A field experiment in a dense inner-city area, *Landscape and Urban Planning*, 2021, **207**, 103998.

17 N. Kabisch, R. Kraemer, O. Masztalerz, J. Hemmerling, C. Püffel and D. Haase, Impact of summer heat on urban park visitation, perceived health and ecosystem service appreciation, *Urban Forestry and Urban Greening*, 2021, **60**, 127058.

18 J. J. Henao, A. M. Rendón and J. F. Salazar, Trade-off between urban heat island mitigation and air quality in urban valleys, *Urban Climate*, 2020, 31, p. 100542.

19 M. Hefny Salim, K. Heinke Schlünzen and D. Grawe, Including trees in the numerical simulations of the wind flow in urban areas: Should we care?, *Journal of Wind Engineering and Industrial Aerodynamics*, 2015, **144**, 84–95.

20 A. Guenther, Biological and Chemical Diversity of Biogenic Volatile Organic Emissions into the Atmosphere, *ISRN Atmospheric Sciences*, 2013, **2013**, 1–27.

21 M. L. Luttkus, E. H. Hoffmann, L. Poulain, A. Tilgner and R. Wolke, The effect of land use classification on the gas-phase and particle composition of the troposphere, *J. Geophys. Res.*, 2022.

22 A. R. Saleem, T. Mahmood, W. Un-Nisa and M. Aslam, Emission and role of biogenic volatile organic compounds in biosphere, *Science Vision*, 2013, 69–78.

23 A. B. Guenther, X. Jiang, C. L. Heald, T. Sakulyanontvittaya, T. Duhl, L. K. Emmons and X. Wang, The Model of Emissions of Gases and Aerosols from Nature version 2.1 (MEGAN2.1): an extended and updated framework for modeling biogenic emissions, *Geosci. Model Dev.*, 2012, **5**, 1471–1492.

24 A. Borbon, H. Fontaine, M. Veillerot, N. Locoge, J. Galloo and R. Guillermo, An investigation into the traffic-related fraction of isoprene at an urban location, *Atmos. Environ.*, 2001, **35**, 3749–3760.

25 S. Reimann, P. Calanca and P. Hofer, The anthropogenic contribution to isoprene concentrations in a rural atmosphere, *Atmos. Environ.*, 2000, **34**, 109–115.

26 A. Panopoulou, E. Liakakou, S. Sauvage, V. Gros, N. Locoge, I. Stavroulas, B. Bonsang, E. Gerasopoulos and N. Mihalopoulos, Yearlong measurements of monoterpenes and isoprene in a Mediterranean city (Athens): Natural *vs.* anthropogenic origin, *Atmos. Environ.*, 2020, **243**, 117803.

27 E. Pallozzi, I. Lusini, L. Cherubini, R. A. Hajiaghayeva, P. Ciccioli and C. Calfapietra, Differences between a deciduous and a conifer tree species in gaseous and particulate emissions from biomass burning, *Environ. Pollut.*, 2018, **234**, 457–467.

28 *Biology, Controls and Models of Tree Volatile Organic Compound Emissions* ed. Ü. Niinemets and R. K. Monson, Springer Netherlands, Dordrecht, 2013, vol. 5.

29 P. Wagner and W. Kuttler, Biogenic and anthropogenic isoprene in the near-surface urban atmosphere–a case study in Essen, Germany, *Sci. Total Environ.*, 2014, **475**, 104–115.

30 J. Jiang, S. Aksoyoglu, G. Ciarelli, E. Oikonomakis, I. El-Haddad, F. Canonaco, C. O'Dowd, J. Ovadnevaite, M. C. Minguillón, U. Baltensperger and A. S. H. Prévôt, Effects of two different biogenic emission models on modelled ozone and aerosol concentrations in Europe, *Atmos. Chem. Phys.*, 2019, **19**, 3747–3768.

31 G. Curci, M. Beekmann, R. Vautard, G. Smiatek, R. Steinbrecher, J. Theloke and R. Friedrich, Modelling study of the impact of isoprene and terpene biogenic emissions on European ozone levels, *Atmos. Environ.*, 2009, **43**, 1444–1455.

32 D. C. Oderbolz, S. Aksoyoglu, J. Keller, I. Barmpadimos, R. Steinbrecher, C. A. Skjøth, C. Plaß-Dülmer and A. S. H. Prévôt, A comprehensive emission inventory of biogenic volatile organic compounds in Europe: improved seasonality and land-cover, *Atmos. Chem. Phys.*, 2013, **13**, 1689–1712.

33 G. Churkina, F. Kuik, B. Bonn, A. Lauer, R. Grote, K. Tomiak and T. M. Butler, Effect of VOC Emissions from Vegetation on Air Quality in Berlin during a Heatwave, *Environ. Sci. Technol.*, 2017, **51**, 6120–6130.

34 H. Hellén, T. Tykkä and H. Hakola, Importance of monoterpenes and isoprene in urban air in northern Europe, *Atmos. Environ.*, 2012, **59**, 59–66.

35 H. Nishimura, H. Shimadera, A. Kondo, K. Akiyama and Y. Inoue, Numerical Analysis on Biogenic Emission Sources Contributing to Urban Ozone Concentration in Osaka, Japan, *AJAE*, 2015, **9**, 259–271.

36 G. Li, R. Zhang, J. Fan and X. Tie, Impacts of biogenic emissions on photochemical ozone production in Houston, Texas, *J. Geophys. Res.*, 2007, **112**, 2131.

37 M. Duane, B. Poma, D. Rembges, C. Astorga and B. Richter Larsen, Isoprene and its Degradation Products as Strong Ozone Precursors in Insubria, Northern Italy, *Atmos. Environ.*, 2002, 3867–3879.

38 A. Guenther, X. Jiang, T. Shah, L. Huang, S. Kemball-Cook and G. Yarwood, in *Air Pollution Modeling and its Application XXVI*, ed. C. Mensink, W. Gong and A. Hakami, Springer Nature Switzerland AG, Cham, 2020.

39 A. Guenther, *A Next Generation Modeling System for Estimating Texas Biogenic VOC Emissions. Final Report. AQRP Project* 16–011, 2017.

40 M. Karl, S.-E. Walker, S. Solberg and M. O. P. Ramacher, The Eulerian urban dispersion model EPISODE. Part II: Extensions to the source dispersion and photochemistry for EPISODE-CityChem v1.2 and its application to the city of Hamburg, *Geosci. Model Dev. Discuss.*, 2019, 1–62.

41 A. Bastos, P. Ciais, P. Friedlingstein, S. Sitch, J. Pongratz, L. Fan, J. P. Wigneron, U. Weber, M. Reichstein, Z. Fu, P. Anthoni, A. Arneth, V. Haverd, A. K. Jain, E. Joetzjer, J. Knauer, S. Lienert, T. Loughran, P. C. McGuire, H. Tian, N. Viovy and S. Zaehle, Direct and seasonal legacy effects of the 2018 heat wave and drought on European ecosystem productivity, *Sci. Adv.*, 2020, **6**, eaba2724.

42 B. Schuldt, A. Buras, M. Arend, Y. Vitasse, C. Beierkuhnlein, A. Damm, M. Gharun, T. E. Grams, M. Hauck, P. Hajek, H. Hartmann, E. Hiltbrunner, G. Hoch, M. Holloway-Phillips, C. Körner, E. Larysch, T. Lübbe, D. B. Nelson, A. Rammig, A. Rigling, L. Rose, N. K. Ruehr, K. Schumann, F. Weiser, C. Werner, T. Wohlgemuth, C. S. Zang and A. Kahmen, A first assessment of the impact of the extreme 2018 summer drought on Central European forests, *Basic Appl. Ecol.*, 2020, **45**, 86–103.

43 DWD, *Klimareport Hamburg*, Offenbach am Main, 2021, **https://www.dwd.de/DE/leistungen/klimareports/ klimareport_hh_2021_download.html**.

44 M. Karl and M. Ramacher, in *Air Pollution Modeling and its Application XXVI*, ed. C. Mensink, W. Gong and A. Hakami, Springer Nature Switzerland AG, Cham, 2020, pp. 235–239.

45 J. D. Fuentes, L. Gu, M. Lerdau, R. Atkinson, D. Baldocchi, J. W. Bottenheim, P. Ciccioli, B. Lamb, C. Geron, A. Guenther, T. D. Sharkey and W. Stockwell, Biogenic Hydrocarbons in the Atmospheric Boundary Layer: A Review, *Bull. Am. Meteorol. Soc.*, 2000, **81**, 1537–1575.

46 A. Guenther, SEASONAL AND SPATIAL VARIATIONS IN NATURAL VOLATILE ORGANIC COMPOUND EMISSIONS, *Ecological Applications*, 1997, **7**, 34–45.

47 M. Karl, A. Guenther, R. Köble, A. Leip and G. Seufert, A new European plant-specific emission inventory of biogenic volatile organic compounds for use in atmospheric transport models, *Biogeosciences*, 2009, **6**, 1059–1087.

48 C. Wu, I. Pullinen, S. Andres, G. Carriero, S. Fares, H. Goldbach, L. Hacker, T. Kasal, A. Kiendler-Scharr, E. Kleist, E. Paoletti, A. Wahner, J. Wildt and T. F. Mentel, Impacts of soil moisture on *de novo* monoterpene emissions from European beech, Holm oak, Scots pine, and Norway spruce, *Biogeosciences*, 2015, **12**, 177–191.

49 H. Rennenberg, F. Loreto, A. Polle, F. Brilli, S. Fares, R. S. Beniwal and A. Gessler, Physiological responses of forest trees to heat and drought, *Plant Biol.*, 2006, **8**, 556–571.

© 2022 The Author(s). Published by the Royal Society of Chemistry

Environ. Sci.: Atmos., 2022, **2**, 1132–1151 | **1149**

50 J. Flexas and H. Medrano, Drought-inhibition of photosynthesis in C3 plants: stomatal and non-stomatal limitations revisited, *Ann. Bot.*, 2002, **89**, 183–189.

51 A. Fortunati, C. Barta, F. Brilli, M. Centritto, I. Zimmer, J.-P. Schnitzler and F. Loreto, Isoprene emission is not temperature-dependent during and after severe drought-stress: a physiological and biochemical analysis, *Plant J. Cell Mol. Biol.*, 2008, **55**, 687–697.

52 R. Atkinson, Atmospheric chemistry of VOCs and NOx, *Atmos. Environ.*, 2000, **34**, 2063–2101.

53 R. Atkinson and J. Arey, Gas-phase tropospheric chemistry of biogenic volatile organic compounds: a review, *Atmos. Environ.*, 2003, **37**, 197–219.

54 M. Karl, K. Tsigaridis, E. Vignati and F. Dentener, Formation of secondary organic aerosol from isoprene oxidation over Europe, *Atmos. Chem. Phys.*, 2009, **9**, 7003–7030.

55 B. Geyer, High-resolution atmospheric reconstruction for Europe 1948–2012: coastDat2, *Earth Syst. Sci. Data*, 2014, **6**, 147–164.

56 EEA, *Urban Adaptation to Climate Change in Europe*, EEA Report, 2012.

57 F. Imbery, K. Friedrich, S. Haeseler, C. Koppe, W. Janssen and P. Bissoli, *Vorläufiger Rückblick auf den Sommer 2018 – eine Bilanz extremer Wetterereignisse*, https://www.dwd.de/DE/leistungen/besondereereignisse/temperatur/20180803_bericht_sommer2018.pdf;jsessionid=1942B5574DB8FDA654C720C27223FB0C.live21062?__blob=publicationFile&v=10.live21062?__blob=publicationFile&v=10, (accessed 1 June 2022).

58 M. Zink, L. Samaniego, R. Kumar, S. Thober, J. Mai, D. Schäfer and A. Marx, The German drought monitor, *Environ. Res. Lett.*, 2016, **11**, 74002.

59 J. Böhm and G. Wahler, *Luftreinhalteplan für Hamburg: 1. Fortschreibung 2012*, 2012, https://www.hamburg.de/contentblob/3744850/f3984556074bbb1e95201d67d8085d22/data/fortschreibung-luftreinhalteplan.pdf.

60 Behörde für Umwelt und Energie, *Luftreinhalteplan für Hamburg (2. Fortschreibung)*, 2017.

61 Anpassungsstrategien an sich verändernde urbane und klimatische Rahmenbedingungen, *Entwicklungskonzept Stadtbäume*, ed. W. Dickhaut and A. Eschenbach, HafenCity Universität Hamburg, Hamburg, 2019, ISBN: 978-3-941722-83-5.

62 EEA, *City Typology*, https://www.eea.europa.eu/themes/sustainability-transitions/urban-environment/sub-sections/urban-green-infrastructure/typology-for-urban-green-infrastructure.

63 R. Köble and G. Seufert, *Novel Maps for Forest Tree Species in Europe*, Torino, Italy, 2001.

64 R. Steinbrecher, A. Lehning and I. Zimmer, Isoprene Synthase Activity and its Relation to Isoprene Emission in *Quercus robur* L., *Plant, Cell Environ.*, 1999, 495–504.

65 J. Kesselmeier and M. Staudt, Biogenic Volatile Organic Compounds (VOC): An Overview on Emission, Physiology and Ecology, *J. Atmos. Chem.*, 1999, 23–88.

66 A. Guenther, T. Karl, P. Harley, C. Wiedinmyer, P. I. Palmer and C. Geron, Estimates of global terrestrial isoprene emissions using MEGAN (Model of Emissions of Gases and Aerosols from Nature), *Atmos. Chem. Phys.*, 2006, 3181–3210.

67 X. Jiang, A. Guenther, M. Potosnak, C. Geron, R. Seco, T. Karl, S. Kim, L. Gu and S. Pallardy, *Isoprene Emission Response to Drought and the Impact on Global Atmospheric Chemistry*, Atmospheric environment, Oxford, England, 2018, 183, pp. 69–83.

68 F. Baret, M. Weiss, R. Lacaze, F. Camacho, H. Makhmara, P. Pacholcyzk and B. Smets, GEOV1: LAI and FAPAR essential climate variables and FCOVER global time series capitalizing over existing products. Part1: Principles of development and production, *Remote Sensing of Environment*, 2013, **137**, 299–309.

69 F. Camacho, J. Cernicharo, R. Lacaze, F. Baret and M. Weiss, GEOV1: LAI, FAPAR essential climate variables and FCOVER global time series capitalizing over existing products. Part 2: Validation and intercomparison with reference products, *Remote Sensing of Environment*, 2013, **137**, 310–329.

70 Slørdal, et al., The Air Quality Information System AirQUIS, *Info. Techn. Environ. Eng*, 2008, 21–33.

71 M. O. P. Ramacher, A. Kakouri, O. Speyer, J. Feldner, M. Karl, R. Timmermans, H. van der Denier Gon, J. Kuenen, E. Gerasopoulos and E. Athanasopoulou, The UrbEm Hybrid Method to Derive High-Resolution Emissions for City-Scale Air Quality Modeling, *Atmosphere*, 2021, **12**, 1404.

72 D. A. Schwarzkopf, R. Petrik, V. Matthias, M. Quante, E. Majamäki and J.-P. Jalkanen, A ship emission modeling system with scenario capabilities, *Atmos. Environ.: X*, 2021, **12**, 100132.

73 U. Pöschl, R. von Kuhlmann, N. Poisson and P. J. Crutzen, Development and Intercomparison of Condensed Isoprene Oxidation Mechanisms for Global Atmospheric Modeling, *J. Atmos. Chem.*, 2000, **37**, 29–52.

74 M. Karl, H.-P. Dorn, F. Holland, R. Koppmann, D. Poppe, L. Rupp, A. Schaub and A. Wahner, Product study of the reaction of OH radicals with isoprene in the atmosphere simulation chamber SAPHIR, *J. Atmos. Chem.*, 2006, **55**, 167–187.

75 R. Bergström, H. A. C. van der Denier Gon, A. S. H. Prévôt, K. E. Yttri and D. Simpson, Modelling of organic aerosols over Europe (2002–2007) using a volatility basis set (VBS) framework: application of different assumptions regarding the formation of secondary organic aerosol, *Atmos. Chem. Phys.*, 2012, **12**, 8499–8527.

76 J. G. Calvert, *The Mechanisms of Atmospheric Oxidation of the Alkenes*, Oxford Univ. Press, New York, 2000.

77 D. Simpson, R. Bergström, A. Briolat, H. Imhof, J. Johansson, M. Priestley and A. Valdebenito, GenChem v1.0 – a chemical pre-processing and testing system for atmospheric modelling, *Geosci. Model Dev.*, 2020, **13**, 6447–6465.

78 J. Zimmermann and D. Poppe, A supplement for the RADM2 chemical mechanism: The photooxidation of isoprene, *Atmos. Environ.*, 1996, **30**, 1255–1269.

79 D. Grosjean, E. Grosjean and E. L. Williams, *Therman Decomposition of C3-Substituted Peroxyacyl Nitrates*, 1994, pp. 447–461.

80 D. J. Barket, A study of the NO x dependence of isoprene oxidation, *J. Geophys. Res.*, 2004, **109**(22), 295.

81 X. Jiang, A. Guenther, M. Potosnak, C. Geron, R. Seco, T. Karl, S. Kim, L. Gu and S. Pallardy, *Isoprene Emission Response to Drought and the Impact on Global Atmospheric Chemistry*, Atmospheric Environment, 2018, pp. 69–83.

82 R. G. Donovan, H. E. Stewart, S. M. Owen, A. R. MacKenzie and C. N. Hewitt, Development and application of an urban tree air quality score for photochemical pollution episodes using the Birmingham, United Kingdom, area as a case study, *Environ. Sci. Technol.*, 2005, **39**, 6730–6738.

83 M. Ma, Y. Gao, Y. Wang, S. Zhang, L. R. Leung, C. Liu, S. Wang, B. Zhao, X. Chang, H. Su, T. Zhang, L. Sheng, X. Yao and H. Gao, Substantial ozone enhancement over the North China Plain from increased biogenic emissions due to heat waves and land cover in summer 2017, *Atmos. Chem. Phys.*, 2019, **19**, 12195–12207.

84 Y. Gao, M. Ma, F. Yan, H. Su, S. Wang, H. Liao, B. Zhao, X. Wang, Y. Sun, J. R. Hopkins, Q. Chen, P. Fu, A. C. Lewis, Q. Qiu, X. Yao and H. Gao, Impacts of biogenic emissions from urban landscapes on summer ozone and secondary organic aerosol formation in megacities, *Sci. Total Environ.*, 2022, **814**, 152654.

85 M. Ma, Y. Gao, A. Ding, H. Su, H. Liao, S. Wang, X. Wang, B. Zhao, S. Zhang, P. Fu, A. B. Guenther, M. Wang, S. Li, B. Chu, X. Yao and H. Gao, Development and Assessment of a High-Resolution Biogenic Emission Inventory from Urban Green Spaces in China, *Environ. Sci. Technol.*, 2022, **56**, 175–184.

86 M. Zhang, C. Zhao, Y. Yang, Q. Du, Y. Shen, S. Lin, D. Gu, W. Su and C. Liu, Modeling sensitivities of BVOCs to different versions of MEGAN emission schemes in WRF-Chem (v3.6) and its impacts over eastern China, *Geosci. Model Dev*, 2021, **14**, 6155–6175.

87 J. Peñuelas, BVOCs: plant defense against climate warming?, *Trends Plant Sci.*, 2003, **8**, 105–109.

88 F. Loreto, P. Pinelli, F. Manes and H. Kollist, Impact of ozone on monoterpene emissions and evidence for an isoprene-like antioxidant action of monoterpenes emitted by Quercus ilex leaves, *Tree Physiol.*, 2004, **24**, 361–367.

89 J. BEAUCHAMP, A. WISTHALER, A. HANSEL, E. KLEIST, M. MIEBACH, U. L. NIINEMETS, U. L. SCHURR and J. WILDT, Ozone induced emissions of biogenic VOC from tobacco: relationships between ozone uptake and emission of LOX products, *Plant, Cell Environ.*, 2005, **28**, 1334–1343.

90 E. Bourtsoukidis, B. Bonn, A. Dittmann, H. Hakola, H. Hellén and S. Jacobi, Ozone stress as a driving force of sesquiterpene emissions: a suggested parameterisation, *Biogeosciences*, 2012, **9**, 4337–4352.

91 A. Peron, L. Kaser, A. C. Fitzky, M. Graus, H. Halbwirth, J. Greiner, G. Wohlfahrt, B. Rewald, H. Sandén and T. Karl, Combined effects of ozone and drought stress on the emission of biogenic volatile organic compounds from Quercus robur L, *Biogeosciences*, 2021, **18**, 535–556.

© 2022 The Author(s). Published by the Royal Society of Chemistry

Environ. Sci.: Atmos., 2022, **2**, 1132–1151 | 1151